Received: October 2024, Accepted: December 2024, Published: December 2024
Digital Object Identifier: https://doi.org/10.34302/CJEE/QSEG2220

DATA DRIVEN RULE-BASED PEAK SHAVING ALGORITHM FOR SCHEDULING REFRIGERATORS

Daniel **KWEGYIR**, Francis Boafo **EFFAH,** Daniel **OPOKU**, Emmanuel Asuming **FRIMPONG**

Department of Electrical and Electronic Engineering, Kwame Nkrumah University of Science and Technology, Kumasi, Ghana.
daniel.kwegyir@knust.edu.gh

Keywords: Thermostatically controlled loads, peak shaving, rule-based algorithm, dynamic flexibility

Abstract*: The increasing use of thermostatically controlled loads (TCLs) like refrigerators poses a significant challenge to the grid due to their potential to increase peak demand. This study introduces a novel rule-based peak-shaving algorithm to effectively manage these loads. The algorithm operates in two modes: day-ahead and real-time. In the day-ahead mode, Long Short-Term Memory (LSTM) neural networks are utilized to forecast demand and generation. A Parameter tuned Grey Wolf Optimizer (GWOP) is proposed and employed to determine the optimal generation for the initial timestep of the scheduling period. The GWOP is tuned using a brute-force grid search method to optimize its parameters. In the real-time mode, the algorithm dynamically adjusts refrigerator operations based on real-time mismatch calculations between predicted demand and generation. Dynamic flexibility thresholds are employed to determine the optimal operation of refrigerators during peak and off-peak periods. This approach aims to minimize energy consumption while maintaining thermal comfort. The algorithm's performance was evaluated using real-world data from the Spanish Transmission Service Operators (TSO). The results demonstrate a significant reduction in peak demand and total energy consumption. The algorithm with dynamic flexibility achieved a substantial 18.89% reduction in peak demand and a notable 12.12% decrease in total energy consumption.*

1. INTRODUCTION

As the world undergoes rapid urbanization and industrialization, electricity demand has surged, especially in developing countries where villages and towns are transforming into urban centers. This increased urbanization, coupled with global warming, has significantly raised the

usage of thermostatically controlled loads (TCLs) such as refrigerators and air conditioners in households and offices [1] Air conditioners account for 14% to 20% of total energy consumption in buildings [2], while refrigerators consume about 10% [1].

The widespread use of TCLs poses a challenge to network stability, particularly in countries with insufficient power generation capacity [3,4]. This can lead to network stress, load shedding, demand-supply mismatches, and increased electricity costs. For consumers, this instability translates into higher costs of consumption, increased cost of economic activities and reduced comfort. Load shedding disrupts daily activities, while demand-supply mismatches drive up electricity prices as utilities purchase power at higher rates or invest in expensive peaking plants. Despite these potential challenges of wide usage of TCLs, they offer advantages for demand-side management (DSM) due to their thermal storage capabilities. Demand-side management strategies can leverage this flexibility to maintain grid stability, reduce operational costs, and ensure a reliable electricity supply. One effective strategy is peak demand shaving, which involves shifting TCL operations to off-peak periods to reduce stress on the power system during peak hours [5,6].

Peak demand shaving has been achieved using energy storage systems (ESS), DSM, and renewable energy integration [7]. Techniques such as optimal appliance scheduling and rule-based methods have been used, with significant work focused on using ESS and heaters for peak management. A simulation on an established building was conducted by [8] to determine the optimal DSM strategy from a building owner's perspective. The analysis revealed that power peak shaving of over 30% could be achieved without significantly impacting indoor conditions. Authors in [9] employed agent-based intelligence to flatten the thermal load of a group of buildings. The work done in [10] utilized a stable roommate’s algorithm to minimize the sum of the thermal requests for 28 buildings in England. However, these studies did not consider the network dynamics in forming the overall district heating thermal request. Authors in [11] used genetic algorithm optimization to minimize the maximum peak value, achieving a 10% reduction in overall thermal demand with minimal schedule variations. Authors in [12] applied the same algorithm for rescheduling, accounting for more significant modifications and the effects of indoor temperature changes. Authors in [13] presented a field test campaign on two district heating networks using the STORM controller, which reduced peaks by 7.5% – 34%, saving operational costs and reducing CO_2 emissions. Authors in [14] developed an active control strategy using a Model Predictive Control algorithm to maximize cogeneration plant profits by using buildings as storage capacity and selling electricity on the spot market at peak prices. Reinforcement Learning (RL) has been marginally used for directly addressing peak demand issues in district heating, typically applied to electric energy peak-shaving. The work done in [15] used an iterative Q-learning algorithm for energy arbitrage and peak-shaving of thermostatically controlled loads in a district heating system. Work done in [16] addressed thermal load management at the building level to reduce thermal peaks while maintaining user

comfort. Demand-side management through multi-agent models to coordinate individual requests and reduce intra-daily fluctuations in thermal demand has also been proposed by [17].

In terms of rule-based approaches for peak shaving, limited research has been done. These mostly involve the use of ESS rather than TCLs. The study in [18] utilized a genetic algorithm (GA) to determine optimal inputs for peak shaving using rule-based method. The proposed optimal rule-based approach was applied to battery scheduling to shape peak. Although the method was effective, the rules employed to develop the proposed rule-based approach were complex and involved a lot of computation. Authors in [19] introduced a real-time battery management algorithm for peak demand shaving for commercial buildings. However, the work did not account for a dynamic demand limit that can be adjusted to meet various peak requirements for commercial buildings. Additionally, studies done in [20–22] evaluated peak shaving control with battery scheduling, considering a fixed demand limit. The fixed limits presented tight tolerance for the algorithms to operate leading to the creation of additional peaks and increased energy consumption. Again, the study carried out in [23] considered a dynamic demand limit for the peak shaving method. However, the method was specifically applied to Malaysian commercial buildings. Authors in [24] considered a battery controller with a fixed demand limit for peak shaving but did not maintain flexibility in day-to-day management.

Although a good amount of work has been done on peak shaving involving TCLs, ESS and renewables, there are some existing gaps. The literature mostly focuses on optimizing thermal loads and minimizing thermal requests without considering the network dynamics and their impact on overall thermal demand. Methods such as those using genetic algorithms (GA) for peak shaving (e.g., [11], and [25]) and the complex rule-based approaches for battery scheduling (e.g., study [18]) involve significant computational complexity which may not be feasible for real-time or resource-constrained environments. Many studies, including those by [14] have applied fixed demand limits or static control strategies. Even though some works (e.g., study [23]) considered dynamic demand limits, they were context-specific (e.g., applied to Malaysian commercial buildings) and did not offer a generalizable approach. This work proposes a simple rule-based peak-shaving algorithm with dynamic flexibility thresholds for scheduling refrigerators in real time. The proposed algorithm employs a two-level approach: day-ahead optimization and intra-day real-time adjustments. The research aligns with Goal 7 of the Sustainable Development Goals (SDGs), which aims to ensure access to affordable, reliable, sustainable, and modern energy for all by 2030 [26].

1.1. Research contributions

The research contributions of the paper are outlined below:

A novel rule-based peak shaving algorithm has been proposed to schedule refrigerators, to reduce peak demand. The rule-based algorithm simplifies decision-making by using pre-

defined rules and dynamically adjustable parameters. This reduces the computational complexity of optimization-based approaches like genetic algorithms or multi-objective optimization problems. The proposed algorithm incorporates dynamic flexibility thresholds that adjust based on the system's real-time conditions. This allows for more flexible and efficient management of peak demand.

A data-driven estimation method using smoothing error is proposed to predict future generation in the rule-based algorithm for decision making. The smoothing error method is a statistical technique that uses historical data to smooth out irregularities and provide a more accurate prediction of future generations. This method is integrated into the rule-based algorithm to enhance its predictive capabilities and reduce the computational intensiveness of existing forecasting algorithms.

A simple discrete thermal model of a refrigerator is proposed to simulate the cooling and warming behaviour of refrigerators to test the proposed rule-based algorithm on a case study dataset.

1.2. Structure of paper

The rest of the paper is organized as follows: Section 2 discusses the proposed rule-based peak-shaving algorithm and its sub-control algorithms. Section 3 describes the proposed refrigerator thermal model for the study. The case study dataset used to validate the algorithm's performance is described in Section 4 in addition to the performance metrics employed to assess the algorithm's effectiveness. Section 5 presents the results and discussion. Conclusions and recommendations for future works are discussed in section 6.

2. DESCRIPTION OF PROPOSED RULE-BASED PEAK SHAVING FRAMEWORK AND ALGORITHM

This section presents the proposed data-driven, rule-based peak-shaving algorithm for refrigerators. The proposed framework within which the proposed rule-based peak shaving algorithm runs is given in *Fig. 2*. The framework is designed to run in day-ahead and real-time modes to reduce computational intensity**.** In the day-ahead, a forecast of demand and generation is done using long short-term memory (LSTM). The forecast output is used to identify possible peak and off-peak periods a day-ahead by analyzing the predicted demand against predicted generation using a simple logical algorithm. Again, to make decisions in real-time and reduce computational complexity, an optimization problem is defined to determine the possible optimum generation that the system operator can supply. This is solved with a proposed parameter tunned grey optimizer. The optimum generation is subsequently updated in real time using a smoothing error method.

The proposed rule-based algorithm then takes decision by comparing current demand with updated generation. If a mismatch is detected beyond a certain threshold, the algorithm adjusts the status of refrigerators by either turning them on or off to align demand with available generation capacity. This process continues until the mismatch falls within an acceptable limit. Details of these processes are discussed in the subsequent subsections.

2.1. Forecasting of Day-Ahead Demand and Generation with Long Short-Term Memory Neural Network.

Accurate forecasting of day-ahead demand and generation is crucial for optimizing grid operations and maintaining system stability especially in demand response programs. In this study, a Long short-term memory (LSTM) neural network is employed to forecast the day-ahead demand (P_D') and generation (P_g'). This forecast serves as a fundamental input for the proposed rule-based peak shaving algorithm. The output from the forecast is used to forecast and identify the possible peak and off-peak periods a day-ahead within the real-time scheduling horizon. By analysing the forecasted demand in relation to the forecasted generation, the framework effectively pinpoint the periods of highest and lowest demand beyond a certain margin of the generation, which are classified as peak and off-peak, respectively. These classifications are subsequently fed into the peak shaving algorithm which enables the algorithm to make informed decisions regarding the refrigerator scheduling. This pre-emptive approach helps to reduce real-time computational complexities and enhance the overall efficiency of the algorithm's operations.

The LSTM architecture employed in the study is shown in *Fig. 1* [27]. It is modelled and operated with the forget gate, input gate, candidate cell state, cell state and output gate, described with (1) - (6)**,** respectively. The forget gate (f_t) decides the information to remove from the cell state (c_t), the input gate (i_t) decides which values to update in the cell state, and the candidate cell state ($\widetilde{c_t}$) creates a vector of new candidates' values that could be added to the state, cell state updates by combining the old state and the now candidate values and the output gate (o_t) decides what the next hidden state (h_t) should be, based on the cell state.

$$f_t = \sigma(W_f.[h_{t-1}, x_t] + b_f \quad (1)$$

$$i_t = \sigma(W_i.[h_{t-1}, x_t] + b_i) \quad (2)$$

$$\tilde{c_t} = \tanh(W_C.[h_{t-1}, x_t] + b_c) \quad (3)$$

$$c_t = f_t \odot c_{t-1} + i_t \odot \tilde{c_t} \quad (4)$$

$$o_t = \sigma(W_o.[h_{t-1}, x_t] + b_o) \quad (5)$$

$$h_t = o_t \odot \tanh(c_t) \quad (6)$$

In the LSTM model, x_t is the input data, σ is the sigmoid function, $\tanh$ is the tangent function, *W* and *b* are weight and biases applied during training of the LSTM model respectively.

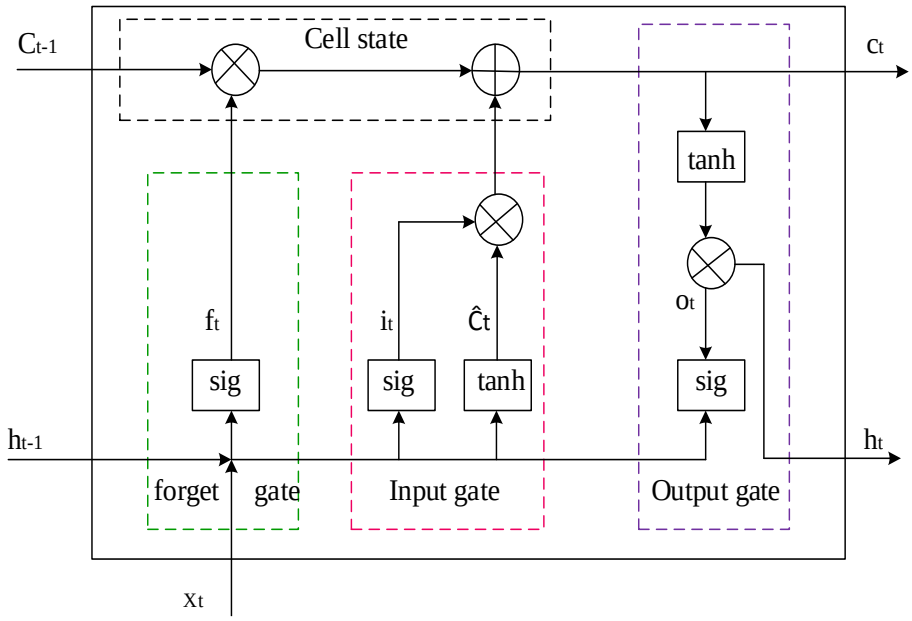

Fig. 1. Architecture of LSTM for forecasting day-ahead demand and generation

Historical time series data $X_t = [x_t^d, x_t^g, x_t^{temp}, x_t^a, x_t^s]$,, including demand (x_t^d), generation (x_t^g), ambient temperature (x_t^{temp}), solar irradiance (x_t^a), and solar power generation (x_t^s), are collected and preprocessed. These variables are critical determinants of demand and generation patterns, providing the LSTM with the necessary context to predict future values accurately. The data is first preprocessed to normalize the values, ensuring that all features contribute equally to the model's learning process. Missing data points are addressed through interpolation, and the dataset is divided into training, validation, and test sets to evaluate the model's performance. During training, the LSTM model is fed sequences of input data spanning multiple time steps, forming an input vector $X_t = [X_t - T + 1, X_t - T + 2, \ldots, X_t]$, or each time t, where T represents the sequence length. The model uses these sequences to predict the target variables—day-ahead demand and generation. The training process involves minimizing mean squared error (MSE) between the predicted demand and generation and their actual values in the training set. The model's parameters (weights and biases) are optimized using backpropagation. The learning rate, batch size, and number of

epochs are carefully tuned to ensure convergence without overfitting. *Fig. 2* provides a flowchart for the method developed to forecast demand and generation.

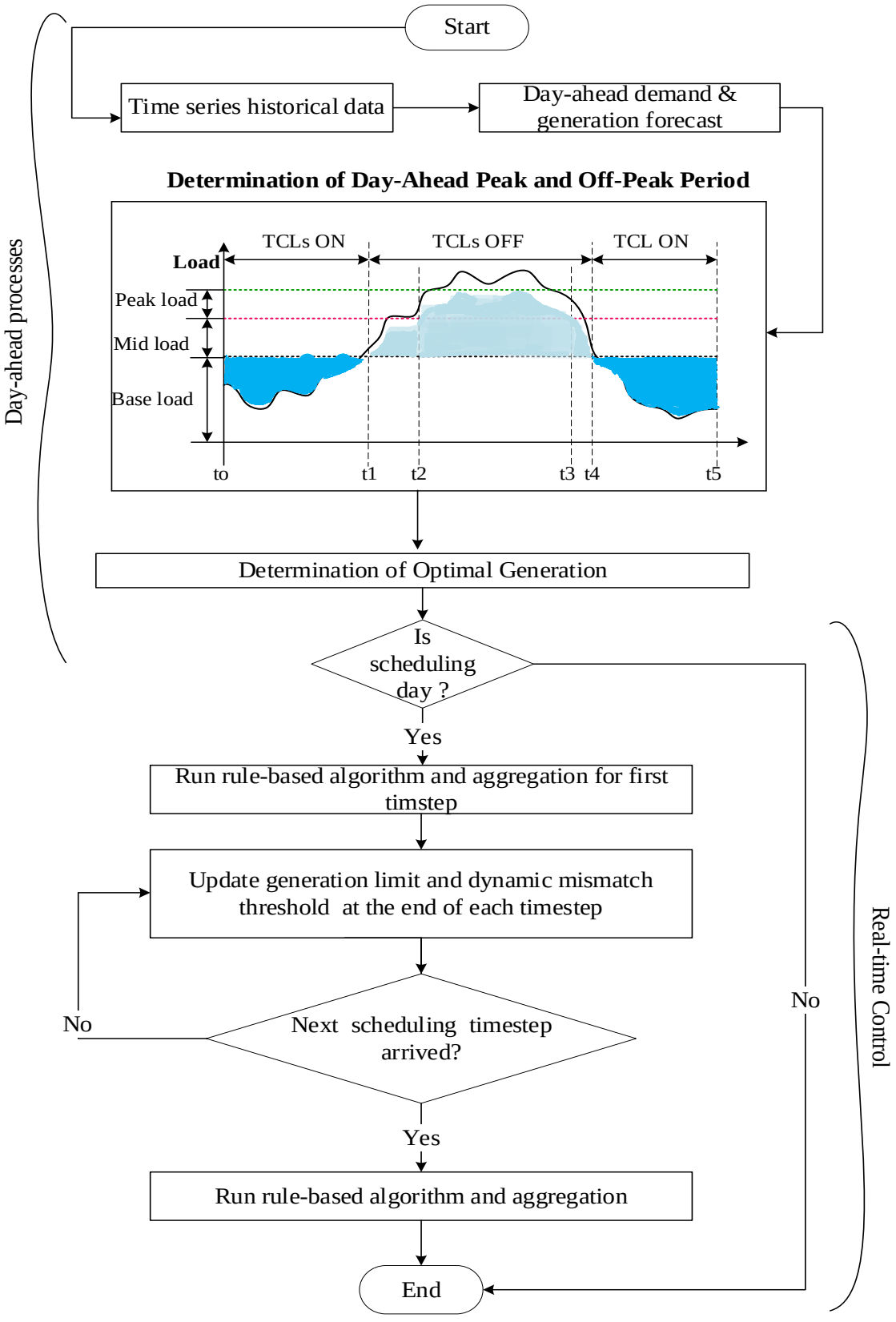

Fig. 2. Proposed data-driven rule-based peak shaving framework

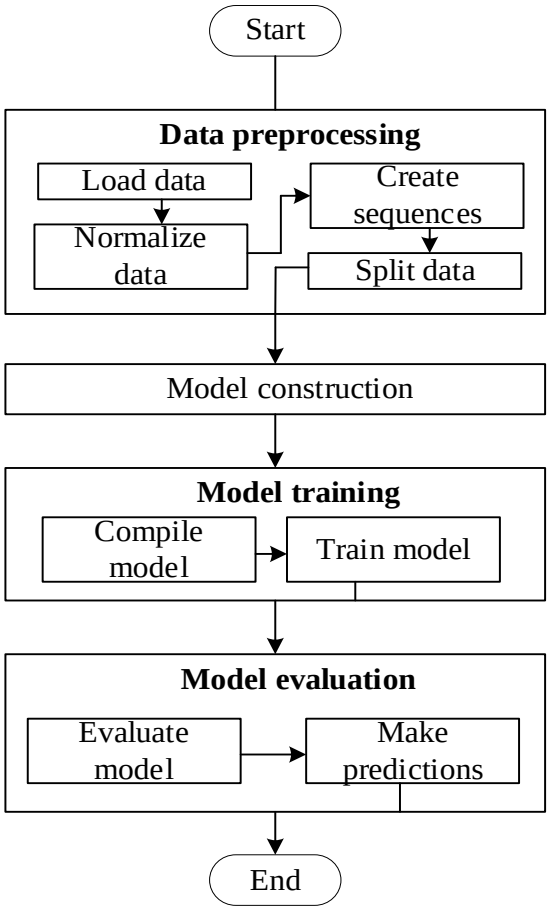

Fig. 3. Flow chart for forecasting demand and generation.

2.2.Determination of Optimal Generation for First Timestep of Scheduling Period

An optimal approach based on historical data is proposed in Algorithm 1 to estimate the potential generation the system operator can produce at the first timestep of the scheduling day (intraday). This enables the proposed rule-based peak-shaving algorithm to make proactive decisions in real-time during the scheduling period without rigorous continuous forecasting at each time step, thereby reducing intensive computation. The optimal generation is denoted as (P_G^l). By accurately estimating the first-time step generation day-ahead, the framework schedules the refrigerators at the first timestep using the proposed rule-based peak shaving algorithm before the actual generation data for the first timestep arrives. This initial (P_G^l) value is subsequently updated in real-time across the scheduling period using a smoothing error method in Algorithm 3.

To determine the first timestep value of (P_G^l) for the scheduling day, an optimization problem is formulated based on historical data on solar power, power demand, and battery discharge data. The objective function of the optimization is formulated in (8), with the optimal generation (P_G^l) as the decision variable. To solve for (P_G^l) , a parameter-tuned grey wolf optimizer (GWOP) based on grid search tunning method is proposed in Algorithm 2. In this

work battery discharge data was not considered in the testing since data was not available. The GWOP finds an optimal value of $\left(P_G^l\right)$ that makes the expression in (8) zero.

$$f\left(P_G^l\right) = \sum_{t=1}^{T} P_D(t) - \left(P_G^l(t) + P_{Solar}(t) + E_{disch}(t)\right) \quad (8)$$

In (8), P_D, P_{Solar} and E_{disch} are power demand, solar power, and battery discharge historical data respectively. The optimization problem is constrained by a lower limit $\left(P_G^l\,(\text{lower})\right)$ and an upper limit $\left(P_G^l\,(\text{upper})\right)$. The lower limit and upper limit are the minimum and maximum generation that can be supplied by the system operator. The pseudocode for determining the optimal generation $\left(P_G^l\right)$ is given in Algorithm 1.

Algorithm. 1. Determination of day-ahead optimal generation

Step	*Start determination of day-ahead optimal generation at first timestep*
1	*Inputs data: historical demand* (P_D)*, historical solar power generation* (P_{solar})
2	*Output: Optimal generated power* (P_G^l)
3	*Solver initialization*
4	*Call objective function based on equation (4.22)*
5	*Set constraints:*
	Lower limit: $P_G^l\ (lower\ )$
	Upper limit: $P_G^l\ (upper)$
6	*Initialize solver and set its parameters*
7	*For* $i = 1$*: number of iterations*
8	*Solve for optimal solution*
9	$i = i + 1$
10	*End For*
11	*Output Optimal solution as* (P_G^l)
12	*End*

2.3. Proposed Parameter Tunned Grey Wolf Optimizer for Determination of Optimal Generation for First Timestep of Scheduling Period

In this paper, a grid search tunning method is employed to tune the classical grey wolf optimizer (GWO) to tune its parameters to enhance the algorithm's performance to solve for the optimal generation limit $\left(P_G^l\right)$. The classical grey wolf is explained below followed by the proposed parameter tuned grey wolf optimizer (GWOP).

2.3.1 Grey Wolf Optimization

The Grey Wolf Optimizer (GWO) [28] is based on the hunting behavior of grey wolves. Grey wolves are social predators that hunt in packs. This hunting behavior enables them to

demonstrate a high degree of cooperation and strategy in their hunting behavior. Each wolf in the pack has a specific role. The alpha (best wolf) wolf leads the hunt, while other members follow its lead and assist in different capacities. The alpha (optimal solution) wolf is the dominant leader, responsible for deciding when and where to hunt. The beta wolf assists the alpha, taking on leadership roles when necessary. The beta wolves represent the second-best solution that help guide the search process and provide a search path for the alpha. Delta wolves assist in hunting and protection. They represent the third-best solution in the search space and support the alpha and beta in the optimization process.

2.3.2. Mathematical Modelling of Metaheuristic Processes of GWO

The hunting mechanism of the grey wolves is characterized by a coordinated and strategic approach that involves several phases. The phases have been discussed below.

Tracking, Chasing, and Approaching the Prey

The wolves track and chase prey, using their sense of smell and hearing to locate it. This is an approach to cautiously get as close as possible to the prey without being detected. The wolves (candidate solutions) encircle the prey by updating their positions based on the distance from the alpha, beta, and delta wolves using (10)**.**

$$\vec{D} = \left|\vec{C} \cdot \vec{X}_p(t) - \vec{X}(t)\right| \tag{9}$$

$$\vec{X}(t+1) = \vec{X}_p(t) - \vec{A} \cdot \vec{D} \tag{10}$$

In the update equation, $\vec{X}(t)$ is the position of a grey wolf, $\vec{X}_p(t)$ is the position of the prey and $\vec{A}$ and $\vec{C}$ are coefficients vectors calculated with (11) and (12).

$$\vec{A} = 2\vec{a} \cdot \vec{r}_1 - \vec{a} \tag{11}$$

$$\vec{C} = 2 \cdot \vec{r}_2 \tag{12}$$

Pursuing and Encircling the Prey

Once the prey is close enough, wolves pursue and encircle it, cutting off escape routes and exhausting the prey. The algorithm simulates encircling behavior by having each wolf adjust its position relative to the positions of the alpha, beta, and delta wolves. This is mathematically modelled to ensure the wolves move closer to the optimal solution. The update equation for this phase is given in (16).

$$\vec{X}_1 = \vec{X}_\alpha - \vec{A}_1 \cdot \left|\vec{C}_1 \cdot \vec{X}_\alpha - \vec{X}\right| \tag{13}$$

$$\vec{X}_2 = \vec{X}_\beta - \vec{A}_2 \cdot \left|\vec{C}_2 \cdot \vec{X}_\beta - \vec{X}\right| \quad (14)$$

$$\vec{X}_3 = \vec{X}_\delta - \vec{A}_3 \cdot \left|\vec{C}_3 \cdot \vec{X}_\delta - \vec{X}\right| \quad (15)$$

$$\vec{X}(t+1) = \frac{\vec{X}_1 + \vec{X}_2 + \vec{X}_3}{3} \quad (16)$$

Attacking the Prey

The wolves attack once the prey is exhausted or cornered, ensuring a successful hunt. The algorithm converges on the optimal solution. As iterations proceed, the search space is exploited more intensively, refining the candidate solutions to converge on the best solution.

2.3.3. Proposed Parameter Tunned Grey Wolf Optimizer

The GWO has been applied to successfully solve numerous optimization problems, however, its performance is sensitive to the algorithm's control parameters; alpha (α), beta (β) and delta (δ) which affects the exploration and exploitation abilities of the wolves. The grid search tunning method is employed to systematically tune the GWO to enhance its exploration and exploration to solve for $\left(P_G^l\right)$. The grid search methods employ a brute-force method to tune the hyper-parameters of the GWO. In the tunning method, a finite set of values for alpha (α), beta (β) and delta (δ) are generated. The GWO is then evaluated for every possible combination of these values. The combination that yields the best performance is selected as the optimal set of parameters finding the optimal value.

2.4. Update of Optimal Generation

In the proposed rule-based peak shaving algorithm, the optimal generation for the second timestep to the end of the scheduling period (T) is updated by accounting for the discrepancy between the actual generation at the first timestep and the historical data on the optimal generation over a time window (w). The proposed update approach utilizes a smoothing error technique [29]. To update the optimal generation $\left(P_G^l\right)$ for the next timestep in the intra-day's decision-making, the error between the actual generation $\left(P_G^{actual}\right)$ at the first timestep and the optimal generation a day before $\left(P_G^l(t-24)\right)$ is calculated over a predefined time window size (w) and averaged. The average error is then added to the first timestep optimal generation $\left(P_G^l(t)\right)$ to determine the next timestep's generation limit for the scheduling period. The update of the optimal generation limit $\left(P_G^l\right)$ is done using (17) - (19). The error (e_t) between the actual generation at the beginning of the current day $\left(P_G^{actual}(t)\right)$ and the optimal generation determined the day before $\left(P_G^l(t-24)\right)$ is calculated using (17). Historical

data on this error is built over the forecasting period to calculate a smoothing error for real-time updates to the optimal generation limit $\left(P_G^l\right)$.

$$e_t = P_G^{actual}(t) - P_G^l(t-24) \tag{17}$$

The smoothing error over a predefined time window size w, is calculated as an average error using (18).

$$\overline{e_t} = \frac{1}{w}\sum_{i=t-w+1}^{t} e_i \tag{18}$$

The optimal generation limit is then updated by (19). The pseudocode in Algorithm 3 provides the detailed steps for the error calculation and generation $\left(P_G^l\right)$ update.

$$P_G^{updated}(t) = P_G^l(t-24) + \overline{e_t} \tag{19}$$

of $\left(P_G^l\right)$. The proposed tunning algorithm is given in Algorithm 2.

Algorithm. 2. Proposed algorithm for tunning grey wolf optimizer

Step	*Start parameter tunning of grey wolf optimizer (GWOP)*
1	*Inputs:*
2	*Parameter ranges for alpha* $\alpha \in [\alpha_{min}, \alpha_{max}]$ *with step size* $\Delta\alpha$
3	*Parameter ranges for alpha* $\beta \in [\beta_{min}, \beta_{max}]$ *with step size* $\Delta\beta$
4	*Parameter ranges for alpha* $\delta \in [\delta_{min}, \delta_{max}]$ *with step size* $\Delta\delta$
5	*Number of iterations T, population size (P), objective function* $f(x)$
6	*Outputs:* α_{opt}, β_{opt}, δ_{opt} *and* f_{best}
7	*For* $i = 1:T$
8	*For alpha* $\alpha \in [\alpha_{min}, \alpha_{min} + \Delta\alpha, \dots, \alpha_{max}]$*:*
9	*For alpha* $\beta \in [\beta_{min}, \beta_{min} + \Delta\beta, \dots, \beta_{max}]$*:*
10	*For alpha* $\delta \in [\delta_{min}, \delta_{min} + \Delta\delta, \dots, \delta_{max}]$*:*
11	*Evaluate GWO with current combinations of* α,β *and* δ
12	*Calculate fitness score* $f_{current}$
13	*End*
14	*End*
15	*End*
16	*If* $f_{current} < f_{best}$
17	*Set* $f_{best} = f_{current}$
18	*Set* $\alpha_{opt} = \alpha$
19	*Set* $\beta_{opt} = \beta$
20	*Set* $\delta_{opt} = \delta$
21	*End if*
22	*End for*
23	*End grid search*

2.5. Identification of Day-Ahead Peak and Off-Peak Periods

In the proposed rule-based peak shaving algorithm, a logical algorithm is proposed in Algorithm 4 to identify peak and off-peak periods within day-ahead forecasted demand data (P_D') relative to day-ahead forecasted generation (P_g'). In the proposed algorithm, peak periods are identified based on the condition that $P_D'(t) > P_g'(t)$ by a certain margin above the system operator's base load. The base load is taken as the optimal generation (P_G^l) across the scheduling period in this work. The algorithm iterates through the dataset at each timestep (t) to identify periods where the demand exceeds generation by the chosen margin. The identified periods are labelled as peak durations and are characterized by their start and end times. This approach allows the algorithm to proactively make decisions in real-time based on the forecasted generation rather than waiting for actual generation data to arrive.

Algorithm. 3. Update of optimal generation in real-time

Step	***Start update of generation limit***
1	*Inputs Data*
2	*Define window size (w)*
	Get day-before optimal generation $(P_{G(day-before)}^{l})$
	Get actual generation (P_G^{actual})
3	*Output*
4	*Updated generation limit* $(P_{G(updated)}^{l})$
5	*Smooth error calculation based on averaging window approach*
6	*While current timestep < last timestep of data*
7	*When a new timestep's generation data arrives:*
8	*Calculate error with equation (17)*
9	*If length of error history < w:*
10	*Append error to error history*
11	*Else*
12	*Remove oldest error from history*
13	*Append new error to error history*
14	*End If*
15	*Update generation limit with equation (19)*
16	*Increment current timestep by 1*
17	*Output updated generation* (P_G^l)
18	***End***

Algorithm. 4. Determination of peak and off-peak periods

Step	*Start identification of peak and off-peak durations*
1	*Initialization*
2	*Get forecasted demand data* (P_D')
3	*Get forecasted generation data* (P_g')*.*
4	*Initialize peak durations as an empty list (to store peak durations)*
5	*Set start time to 0 (to track peak starts)*
6	*Loop through demand data*
7	*For* $i = 1$ *to length* (P_D')*:*
8	*If* $P_D'(i) > P_g'(i)$ *by margin:*
9	*If start time == 0, Set start time to i(mark peak start)*
10	*Else if* $P_D'(i) < P_g'(i)$*:*
11	*If start time!= 0, Calculate peak duration and save it in peak*
12	*durations list, the set start time to 0 (reset peak start)*
13	*End If*
14	*End If*
15	*End for*
16	*Handle end-of-Series Peak*
17	*If start time != 0, calculate final peak duration*
18	*End If*
19	*Output*
20	*Print peak durations as "Start Time, End Time" pairs.*
21	*End*

2.6.Proposed Rule-Based Peak Shaving Algorithm

This section discusses the proposed rule-based peak-shaving algorithm for scheduling refrigerators. The algorithm aims to monitor real-time power demand (P_D) and generation (P_G) data to take decisions to align demand with available generation capacity based on predefined rules. The proposed algorithm is shown in *Fig. 4*. The peak and off-peak period controls are given in Algorithm 5, 6, and 7. The decision-making process of the proposed algorithm primarily involves establishing decision making parameter, peak and off-peak period control. During peak periods, the algorithm prioritizes turning OFF refrigerators to shave the peak demand. Conversely, during off-peak periods, the algorithm turns ON refrigerators to balance the overall demand. The algorithm's dynamic adjustment to real-time conditions is a critical feature. It updates the optimal generation (P_G^l) and other decision parameters based on the latest data received to ensure the power system's responsiveness to changing network conditions. Details of the controls within the algorithm are discussed below.

2.6.1. Decision Making Table

The control table for decision-making in the algorithm is given in Table 1. The table summarizes the conditions under which the algorithm operates and the corresponding action to be taken to aggregate the refrigerators. The variable P_D is the demand at current timestep and Y is the mismatch threshold. The mismatch threshold determines the acceptable level of power mismatch during peak and off-peak period control. The variable current refrigerator status ($S^{b}_{i,t}$) is the status of the i^{th} refrigerator at time t, where 0 indicates OFF and 1 indicates ON. The variable new refrigerator status ($S^{n}_{i,t}$) is the new status of the i^{th} refrigerator at time t determined by the algorithm`s control logic. Finally, the action description shows the action taken by the algorithm based on the current system conditions.

Table 1. Peak and Off-Peak Decision-Making Conditions

Condition Check	**Control Condition**	**Current Refrigerator Status ($S^{b}_{i,t}$)**	**New Refrigerator Status ($S^{n}_{i,t}$)**	**Action Description**
Peak period && $(P'_D) > (P^{l}_G)$	If mismatch threshold (Y) is exceeded	0 (OFF)	0 (OFF)	Maintain TCL OFF
Peak period && $(P'_D) > (P^{l}_G)$	If mismatch threshold (Y) is exceeded	1(ON)	0 (OFF)	Turn OFF TCL
Peak period && $(P'_D) \leq (P^{l}_G)$	If mismatch threshold (Y) is not exceeded	Any	Any	Maintain status
Off peak period && $(P'_D) < (P^{l}_G)$	If mismatch threshold (Y) is exceeded	1 (ON)	1 (ON)	Maintain TCL ON
Off peak period && $(P'_D) < (P^{l}_G)$	If mismatch threshold (Y) is exceeded	0 (OFF)	1 (ON)	Turn ON TCL
Off peak period && $(P'_D) \geq (P^{l}_G)$	If mismatch threshold (Y) is not exceeded	Any	Any	Maintain status

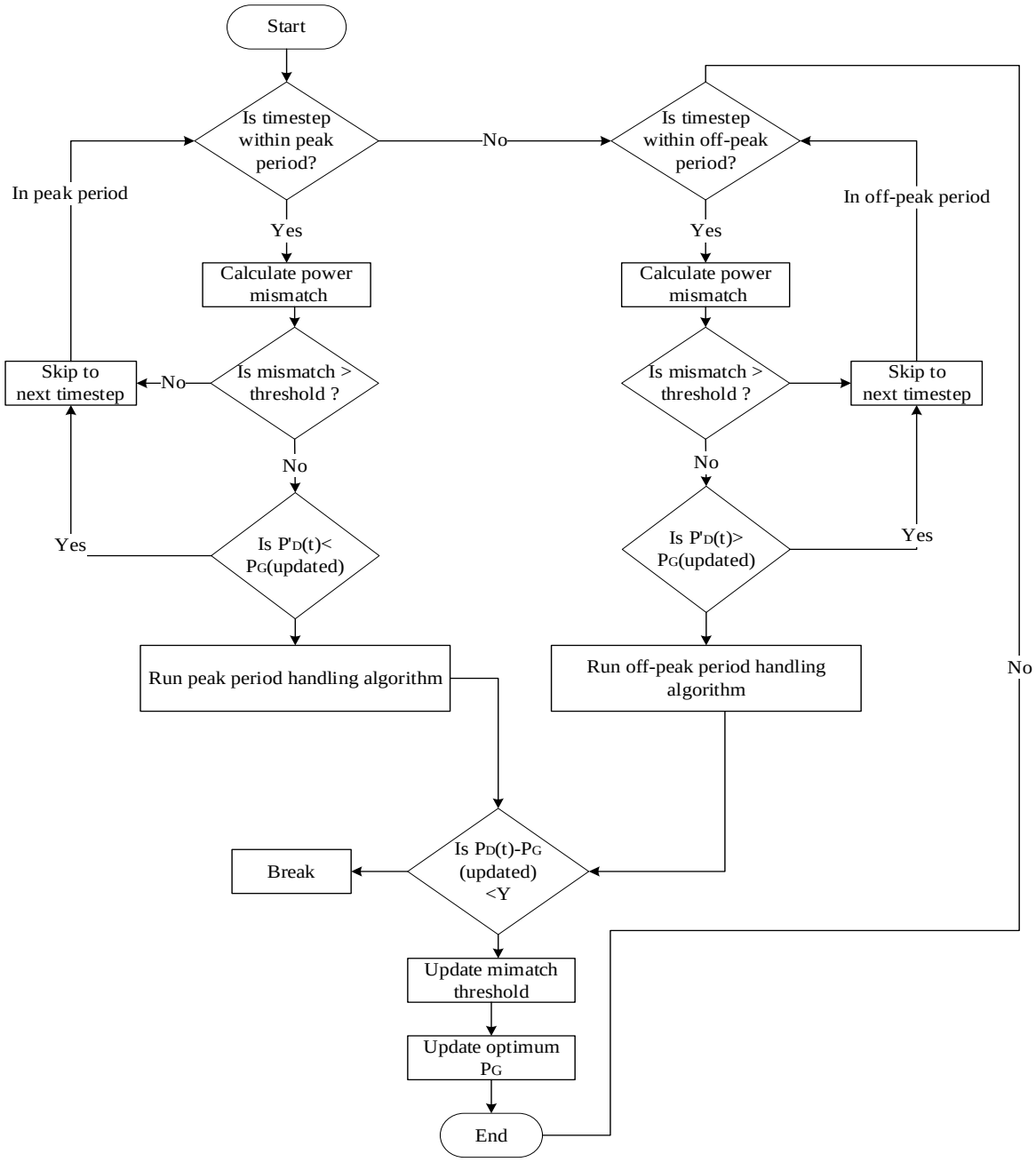

Fig. 4.Proposed rule-based peak shaving algorithm

2.6.2. Algorithm Initialization

The proposed rule-based peak shaving algorithm is initialized as follows:

Step	*Initialize algorithm*
1	*Get real-time demand* $P_D(t)$
2	*Get history of previous optimal generation* (P_G^l)
3	*Run LSTM forecast and output* (P_D') *and* (P_g'),
4	*Run Algorithm 1: output optimal generation at first timestep* (P_G^l)

Step	*Initialize algorithm*
5	*Run Algorithm 4 on step 3: output peak and off-peak periods.*
6	*Get critical temperature ($\theta_{critical}$)*
7	*Get current compartment temperatures of all refrigerators: θ_c*

2.6.3. Peak Period Handling

During th**e** peak periods, the algorithm's rules are designed to reduce the demand to stay close to the real time generation (P_G) by turning OFF as many refrigerators as possible. The number of refrigerators to be turned off by the algorithm is limited by the mismatch threshold (Y) . This action helps to shave the peak demand and prevent grid overload. The peak period control and decision-making steps are provided in Algorithm 5.

Algorithm 5. Peak period handling

Step	*Start peak period control and aggregation*
1	*If t is within a peak period:*
2	*Calculate power mismatch=$\left\|P'_D(t) - P^l_G(t)\right\|$*
3	*If $P'_D(t) > P^l_G(t)$,*
4	*If current power mismatch >Y: If no skip to the next timestep.*
5	*Else*
6	*For i=1 to N: // start aggregation*
7	*If $S^b_{i,t}$=0, set new status: $S^n_{i,t}$=$S^b_{i,t}$*
8	*Else set new status: $S^n_{i,t}$=0*
9	*Begin warming of refrigerator i*
10	*Start waiting time for next schedule of refrigerator i*
11	*Update aggregated demand: $P_D(t) = P_D(t) + S^n_{i,t}.P_r$*
12	*If $\left\|P_D(t) - P'_g(t)\right\| < Y$, break // stop aggregating*
13	*Update mismatch threshold Y*
14	*Update $P^l_G(t)$*

2.6.4. Off-Peak Period Handling

During the off-peak periods, the algorithm's rules are designed to turn ON refrigerators to increase the demand by utilizing the excess generation and preventing generation from going to waste. The off-peak period controls and decision-making steps are provided in *Algorithm 6.*

Algorithm 6. Off-peak period handling

Step	*Start off-peak period control and aggregation*
1	*If t is within off-peak period:*

Step	*Start off-peak period control and aggregation*
2	*Calculate power mismatch=*$\left\|P'_D(t) - P^l_G(t)\right\|$
3	*If* $P'_D(t) < P^l_G(t)$
4	*If current power mismatch >Y: If no skip to the next timestep.*
5	*Else*
6	*For* i*=1 to N:* *// (start aggregation)*
7	*If* $S^b_{i,t}$*=1, set new status:* $S^n_{i,t}=S^b_{i,t}$
8	*Else set new status:* $S^n_{i,t}=1$
9	*Begin cooling of refrigerator* i
10	*Start waiting time for next schedule of refrigerator* i
11	*Update aggregated demand:* $P_D(t) = P_D(t) + S^n_{i,t}.P_r$
12	*If* $\left\|P_D(t) - P'_g(t)\right\| < Y$*, break* *// (stop aggregating)*
13	*Update mismatch threshold Y*
14	*Update* $P^l_G(t)$

2.6.5. Proposed Dynamic Mismatch Threshold

In the proposed rule-based algorithm, a dynamic adjustment is employed based on system conditions to adjust the mismatch threshold. A dynamic adjustor based on sigmoid function is proposed to smoothly adjust the mismatch threshold at each timestep based on the difference between actual generation at the previous timestep $(\mathrm{P_G(t-1)})$ and actual demand at the previous timestep $(\mathrm{P_D(t-1)})$. The dynamic thresholding method ensures that the algorithm adapts to changing system conditions more effectively to maintain a balance between demand and supply while avoiding the pitfalls of too tight or too loose thresholds. The sigmoid function provides smooth and continuous adjustment to prevent abrupt changes in refrigerator operation that could lead to instability. The dynamic adjustment is formulated in equation (20).

$$\mathrm{Y(t) = Y_{base}(t) + \frac{1}{1+e^{-k\left(P_G(t-1)-P_D(t-1)\right)}}} \tag{20}$$

where $\mathrm{Y(t)}$ is the mismatch threshold and $\mathrm{Y_{base}(t)}$ is the base mismatch selected by the system operator.

3. SIMULATION OF REFRIGERATOR COOLING AND WARMING BEHAVIOUR FOR TESTING PROPOSED RULE-BASED ALGORITHM

The discrete thermal model of a vapor compressor refrigeration system (VCRS) is employed to simulate cooling and warming of refrigerator compartment in the testing phase of

the proposed rule-based peak shaving algorithm. The discrete models of the warm-up and cool-down of the refrigerator compartment are given by equation (21) and (22) respectively.

$$\theta_c(t+\Delta t) = \left(1 - \frac{\Delta t}{C_L.R_i}\right).\theta_c(t) + \frac{\Delta t}{C_L.R_i}.\theta_a\,(t) \tag{21}$$

$$\theta_c(t+\Delta t) = \left(1 - \frac{\Delta t}{C_L.R_i}\right).\theta_c(t) + \frac{\Delta t}{C_L.R_i}.\theta_a\,(t) + \frac{\Delta t}{C_L.R_e}.\theta_e(t) \tag{22}$$

where θ_c is the cabinet temperature at time t, C_L is the heat storage capacity of cabinet, θ_a is the ambient temperature at time t, R_i is the thermal resistance of the insulation and θ_e is the evaporator temperature.

The cooling and warming behavior of the refrigerator is achieved with the controls in equation (23) where $\theta_{critical}$ is the set threshold temperature. In the control, when $S = 1$, the refrigerator is turned ON and when $S = 0$ the refrigerator is turned OFF.

$$\theta_c(t+\Delta t) = \begin{cases} \text{Cool}, & \theta_c(t) > \theta_{critical}, S = 1 \\ \text{Warm}, & \theta_c(t) < \theta_{critical}, S = 0 \end{cases} \tag{23}$$

The refrigerator power consumption is modelled according to equation (24). The refrigerator consumes rated power (P_r) when the compressor is ON and 0 when OFF.

$$P_{in}(t) = \begin{cases} 0 & , \ S = 0 \\ P_r & , \ S = 1 \end{cases} \tag{24}$$

The total power drawn by all the refrigerators within a timestep is given by equation (25).

$$P_{total}(t) = \sum_{t=1}^{T}\sum_{i=1}^{N} S_{i,t}P_{in}^{i}(t) \tag{25}$$

Algorithm 7 is used to simulate the thermal behavior of the refrigerators.

Algorithm 7. Simulation of thermal behavior of multiple refrigerators

Step	*Start simulation of thermal behavior of TCLs*	
1	*Inputs*	
2	*Number of refrigerators (N)*	
3	$\theta_c^0 = [1, \dots, M]$	*// initial compartment temperature*
4	$\theta_a^0 = [1, \dots, M]$,	*// initial ambient temperature*
5	$\theta_e^0 = [1, \dots, M]$,	*// initial evaporator temperature*

Step	*Start simulation of thermal behavior of TCLs*
6	Δt *// time step*
7	*Initialize all other parameters:* θ_{ref}, P_r
8	*Simulation duration (T).*
9	*Outputs:*
10	θ_c, *Pin*
11	*Main loop*
12	*For* Δt *=1: T*
13	*For* $i = 1$: *M*
14	*If* $\theta_c(t) < (\theta_{ref})$
15	*Turn OFF*
16	*Update compartment temperature using equation (22)*
17	*Update refrigerator power (Pin) using equation (24)*
18	*Else*
19	*Turn ON*
20	*Update compartment temperature using equation (23)*
21	*Update refrigerator power (Pin) using equation (24)*
22	*End if*
23	*End for*
24	*End for*
25	*End algorithm*

4. DESCRIPTION OF CASE STUDY SYSTEM, SIMULATION AND TESTING

The study utilizes a dataset from Spanish Transmission Service Operators (TSO) spanning four years (2015-2018) [30] to test the proposed rule-based peak-shaving algorithm for scheduling refrigerators. The data includes electricity consumption, pricing, generation, and weather information. A unique aspect of this dataset is its granularity, offering hourly records for each variable. This level of detail is essential for accurately modelling and simulating the dynamic behavior of electricity demand and supply, which is critical for the study. The generation data comprises renewable energy sources i.e, solar and conventional energy sources i.e, thermal and geothermal. This mix of generation types allows for rigorous performance testing of the algorithm in a realistic and varied energy landscape.

All generation sources except solar are combined as total generation to determine the optimal generation limit using Algorithm 1. The data mainly consist of hourly demand data. To test the scheduling ability of the algorithm, 30% of the hourly demand at each timestep is simulated as refrigerator demand to be scheduled. In the testing, 1000 refrigerators are simulated to represent the 30% demand at each hour. The unit maximum power consumption

when a refrigerator is ON across the 48-hour period is given in *Fig. 5*. The day-ahead demand and generation forecast is done for December 30, 2018, and December 31, 2018. The optimal generation is determined for the first hour of December 30, 2018.

Simulations were conducted on an Intel(R) Core (TM) i7-6600U CPU @ 2.60GHz 2.81 GHz with 20.0 GB (19.9 GB usable) RAM using MATLAB simulation software. The parameters for simulating the rule-based peak shaving algorithm are given in Table 2.

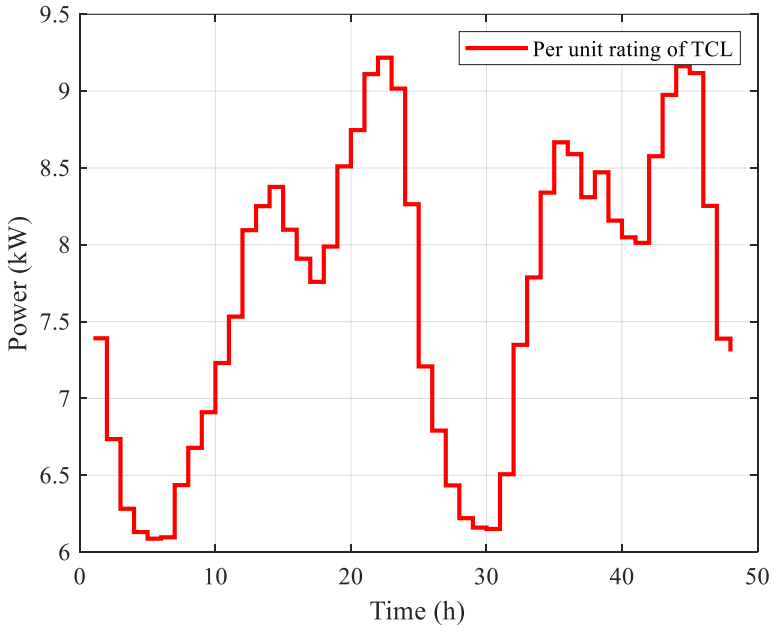

Fig. 5. Per unit rating of TCLs when ON for scheduling

Table 2. Simulation parameters

Parameter	**Value**
P_G^l (lower)	0 MW
P_G^l (upper)	Maximum historical generation
T	48 hours
Refrigerator power rating when ON (P_r)	Based on Figure 4
Mismatch sensitivity levels	0 kW, 500 kW, dynamic mismatch
Population size of PGWO	100
Number of refrigerators	1000
Baseline status	Randomly generated
$\theta_{critical}$	5 ℃
C_L	1000 kW/℃
R_i	0.98℃/kW
R_e	0.09℃/kW
Waiting time	20 Minutes
Margin of identifying peak periods	Demand exceeds generation by 5%

Parameter	**Value**
Base load for mismatch	500 kW
θ_e	Randomly simulated around -2℃
θ_a	Real weather data for scheduling period
Initial compartment temperature of refrigerators	Randomly generated
Batch Size	64
Epochs	1000
Learning rate	0.01

4.1. Performance Evaluation Metrics

To assess the performance of the proposed peak-shaving algorithm, the following metrics are considered.

4.1.1. Peak Demand Reduction

Peak demand reduction measures the extent to which the algorithm successfully reduces the highest electricity demand peaks during peak periods. It is calculated as the percentage decrease in peak demand after implementing the algorithm compared to the initial peak demand given by equation (26).

$$\text{Peak Demand Reduction } (\%) = \frac{(\text{Peak Demand Before} - \text{Peak Demand After})}{\text{Peak Demand Before}} \quad (26)$$

4.1.2. Energy Consumption

The energy consumption analysis compares the total energy consumption before and after implementing the peak demand shaving algorithm. It assesses whether the algorithm effectively manages energy usage and leads to overall energy savings. Equation (27) is used to calculate the energy consumption increase or decrease.

$$\text{Energy Consumption Increase } (\%) = \frac{(\text{Total Energy Consumption After} - \text{Total Energy Consumption Before})}{\text{Total Energy Consumption Before}} \quad (27)$$

4.1.3. Demand-Supply Mismatch

Demand-supply mismatch metric quantifies the deviation between electricity demand and supply at any given time. It evaluates how well the algorithm balances demand and supply to minimize mismatches. This is calculated with equation (28) is used to calculate the demand and supply mismatch at each timestep during the scheduling period.

$$\text{Demand} - \text{Supply Mismatch} = |\text{Demand} - \text{Supply}| \quad (28)$$

4.1.4. TCL Status Changes

The TCL status changes metric refers to the frequency and magnitude of changes in the operating status (ON/OFF) of the TCLs in response to the algorithm's instructions. It evaluates the algorithm's ability to manage appliance operation efficiently while maintaining user comfort and minimizing disruptions. Equation (29) is used to calculate the total status changes of TCL during the scheduling period.

$$\text{Total Status Changes} = \sum_{i=1}^{N} \left| S_{i,t}^{b} - S_{i,t}^{n} \right| \quad (29)$$

5. RESULTS AND DISCUSSIONS

This section presents discussions of the results obtained from implementing the proposed rule-based peak demand-shaving algorithm. The discussions focus on the impact of different scenarios of flexibility levels on the proposed algorithm's effectiveness in peak shaving. The effectiveness is assessed based on peak demand reduction, total energy consumption reduction, refrigerator switching frequency, and the average mismatch between demand and supply. The results highlight the benefits and limitations of offering strict and dynamic flexibility into optimizing demand response programs.

5.1. Scenario 1: Strict Flexibility Threshold

The results of applying the proposed rule-based peak shaving algorithm with strict mismatch threshold is presented in Table 3. This scenario is simulated to assess the algorithm's effectiveness for matching the demand exactly to the available generation at each timestep.

Table 3. Performance Metrics for Strict Flexibility Threshold Scenario

Performance Metric	**Value**
Peak Demand Before	30619.00 MW
Peak Demand After	25107.83 MW
Peak Demand Reduction	18.00%
Total Energy Consumption Before	1228351.00 MWh
Total Energy Consumption After	1088485.3778 MWh
Energy Consumption decrease	11.39%
Total Status Changes in Refrigerators	13000 times
Average Demand-Supply Mismatch	693.99 kW

Following the application of the proposed peak shaving algorithm, the peak demand was reduced from 30,619.00 MW to 25,107.83 MW, representing a significant reduction of 18.00%. This notable decrease demonstrates the algorithm's effectiveness in managing and lowering peak electricity demand, which is crucial for mitigating the need for costly peaking power plants, alleviating stress on the power grid, and potentially reducing electricity costs for consumers. Additionally, the total energy consumption decreased by 11.39%, from 1,228,351.00 MWh to 1,088,485.38 MWh. This substantial reduction in energy consumption, a key indicator of the algorithm's effectiveness, highlights its ability to manage peak demand and achieve significant overall energy savings, which can contribute to more sustainable energy use and lower operational costs. However, the algorithm's strict mismatch threshold led to a high switching quantified in terms of total status changes in the refrigerators, with 13,000 status changes recorded. Each status change reflects a switch between ON and OFF states. While this frequent switching indicates the algorithm's responsiveness to maintain a tight balance between supply and demand, it may also pose a risk of increased wear and tear on the appliances, potentially reducing their lifespan and increasing maintenance costs. The average demand-supply mismatch was 693.99 kW, reflecting the deviation between scheduled demand and available generation over the scheduling period. This mismatch arises due to the inherent difficulty in perfectly aligning demand with supply at every timestep, especially under the high variability of system conditions and the frequent switching triggered by the stringent mismatch threshold.

Fig. 6 provides a detailed comparison of the scheduled demand, unscheduled demand, actual generation, and the updated optimum generation over the scheduling period, illustrating the performance of the peak shaving algorithm under the strict flexibility threshold.

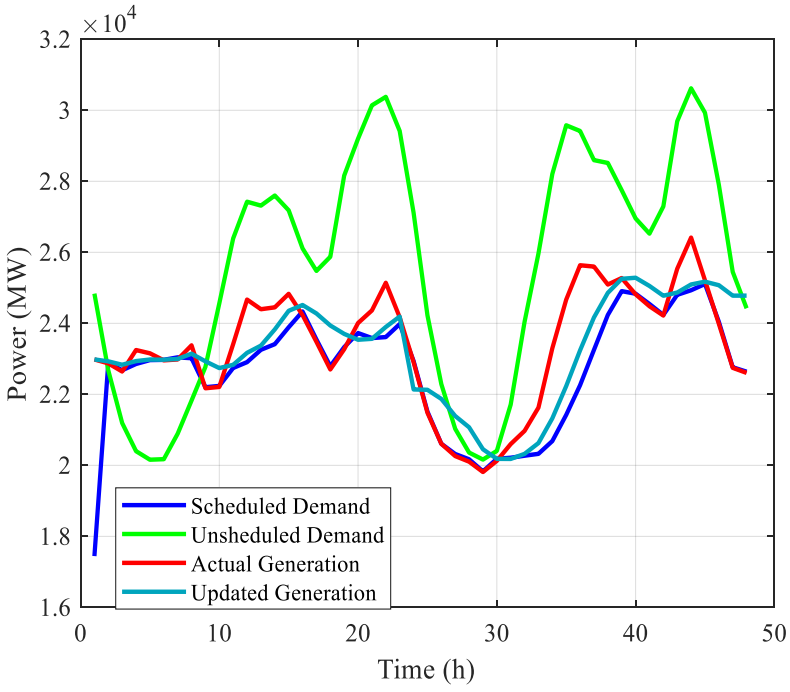

Fig. 6. Comparison of scheduled and unscheduled demand under strict flexibility threshold

5.2. Scenario 2: Base load as flexibility Threshold

The results of applying the proposed rule-based peak shaving algorithm with a flexibility threshold of 500 kW across the scheduling period is presented in Table 4. This scenario is simulated to assess the algorithm's effectiveness under some level of flexible threshold.

Table 4. Performance Metrics for Base Load Flexibility Threshold Scenario

Performance Metric	**Value**
Peak Demand Before	30619.00 MW
Peak Demand After	24852.08 MW
Peak Demand Reduction	18.83%
Total Energy Consumption Before	1228351.00 MWh
Total Energy Consumption After	1081227.60 MWh
Energy Consumption decrease	11.98%
Total Status Changes in Refrigerators	3006 times
Average Demand-Supply Mismatch	1118.64 kW

After applying the peak shaving algorithm with a base load flexibility threshold, the peak demand was reduced from 30,619.00 MW to 24,852.08 MW, achieving an 18.83% reduction. This result shows a slightly higher peak demand reduction compared to the strict flexibility threshold scenario, with an additional reduction of 0.83%. This suggests that incorporating a flexibility limit can enhance the algorithm's effectiveness in reducing peak demand, allowing for more adaptable management of power usage. The total energy consumption after scheduling decreased by 11.98%, from 1,228,351.00 MWh to 1,081,227.60 MWh. This is a marginal improvement over the strict flexibility threshold scenario, indicating that the use of a base load flexibility threshold not only maintains peak demand reduction but also results in greater overall energy savings. Moreover, the total number of status changes for refrigerators dropped significantly to 3,006. This is a substantial reduction compared to the strict flexibility scenario, indicating less frequent switching of TCLs. The decrease in switching events implies reduced wear and tear on appliances, potentially extending their lifespan and lowering maintenance costs, thereby highlighting the financial benefits of incorporating a flexibility threshold. However, the average demand-supply mismatch in this scenario increased to 1,118.64 kW. This higher mismatch suggests that while the flexibility allowance effectively reduces peak demand and energy consumption, it comes at the expense of a less precise alignment between demand and supply. This misalignment could lead to more frequent periods of surplus or deficit, impacting the overall efficiency of energy distribution.

Fig.7 compares the scheduled demand, unscheduled demand, actual generation, and updated optimum generation over the scheduling period, showcasing the impact of using a base load flexibility threshold on the peak shaving algorithm's performance.

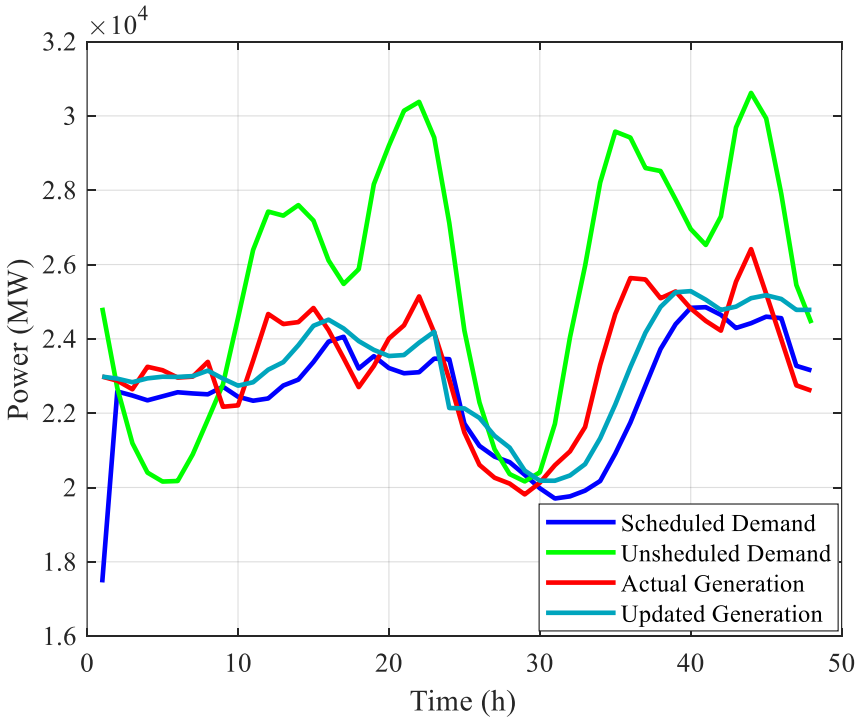

Fig. 7. Comparison of scheduled and unscheduled demand under base load flexibility threshold

5.3.Scenario 3: Proposed Dynamic Flexibility Threshold

The performance of the proposed rule-based peak shaving algorithm with dynamic flexibility thresholds is presented in Table 5. This scenario evaluates the effectiveness of the algorithm when the mismatch thresholds change dynamically based on system conditions.

Table 5. Performance Metrics for Dynamic Flexibility Threshold Scenario

Performance Metric	**Value**
Peak Demand Before	30619.00 MW
Peak Demand After	24845.19 MW
Peak Demand Reduction	18.89%
Total Energy Consumption Before	1228351.00 MWh
Total Energy Consumption After	1079489.82 MWh
Energy Consumption decrease	12.12%
Total Status Changes in Refrigerators	3006 times
Average Demand-Supply Mismatch	1012.41 kW

Applying dynamic flexibility thresholds led to a peak demand reduction of 18.89%, lowering the peak demand from 30,619.00 MW to 24,845.19 MW. This is the highest peak demand reduction observed across all scenarios, surpassing the strict mismatch threshold (18.00%) and the 500 kW flexibility threshold (18.83%). The results indicate that dynamic flexibility thresholds enhance the algorithm's ability to manage and reduce peak demand more effectively by adapting to real-time system conditions. Total energy consumption decreased by 12.12%, from 1,228,351.00 MWh to 1,079,489.82 MWh. This represents the most significant reduction in energy consumption among all scenarios, outperforming both the strict mismatch threshold (11.39%) and the 500 kW flexibility limit (11.98%). The greater decrease in energy consumption under the dynamic threshold scenario underscores the improved overall energy efficiency achieved by adjusting the thresholds dynamically. The total number of status changes for refrigerators was 3,006, consistent with the 500 kW flexibility threshold scenario and significantly lower than the 13,000 status changes observed in the strict mismatch threshold scenario. This consistency in status changes indicates that both the dynamic and base load flexibility thresholds can maintain refrigerator operations more reliably, reducing frequent switching and potentially lowering wear and tear and maintenance costs. The average demand-supply mismatch for the dynamic flexibility threshold scenario was 1,012.41 kW. While this is lower than the mismatch observed with the 500 kW flexibility limit (1,118.64 kW), it is higher than the mismatch in the strict mismatch threshold scenario (693.99 kW). This suggests that although the dynamic flexibility thresholds improve peak shaving and energy efficiency, it introduces a certain level of mismatch between demand and supply. However, the mismatches are within acceptable ranges.

Fig. 8 compares the scheduled demand, unscheduled demand, actual generation, and updated optimum generation over the scheduling period, illustrating the impact of dynamic flexibility thresholds on the performance of the peak shaving algorithm.

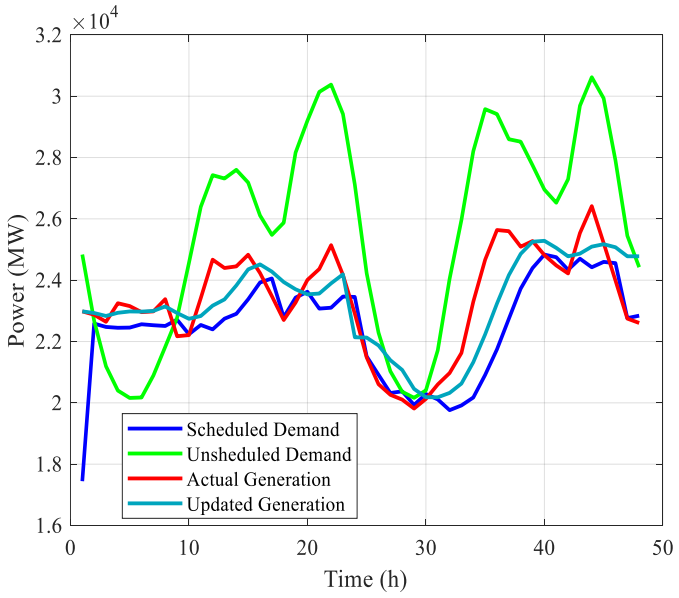

Fig. 8. Comparison of scheduled and unscheduled demand under dynamic flexibility threshold

Fig. 9 provides a comparison of scheduled demand across the three flexibility threshold scenarios: strict (0 kW), base load, and dynamic flexibility thresholds. The mismatches across the three flexibility threshold scenarios: strict (0 kW), base load, and dynamic flexibility thresholds are compared in *Fig 10*. This comparison helps to highlight how each approach impacts demand scheduling, particularly during peak periods.

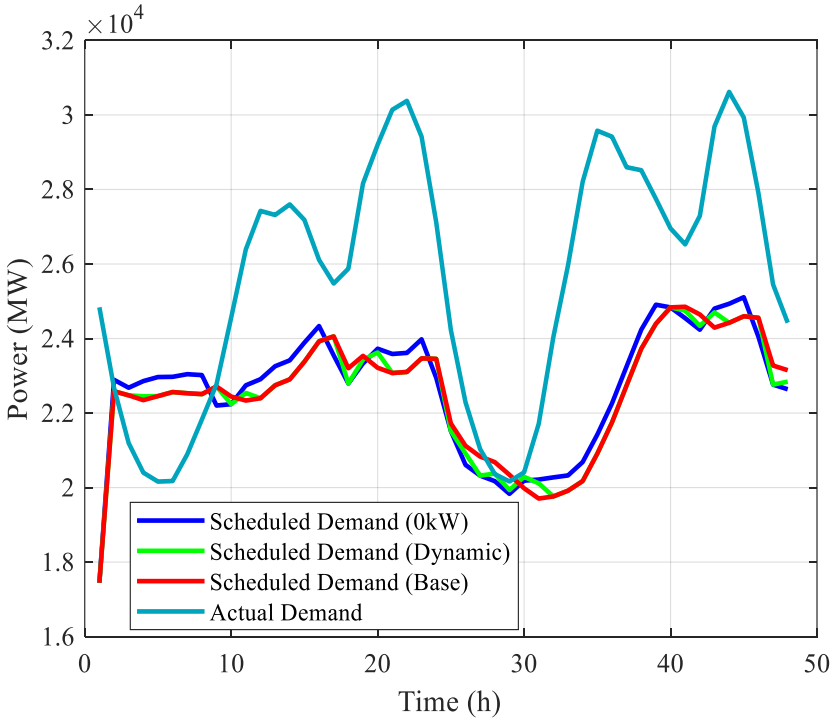

Fig. 9. Comparison of scheduled demand for different scenarios

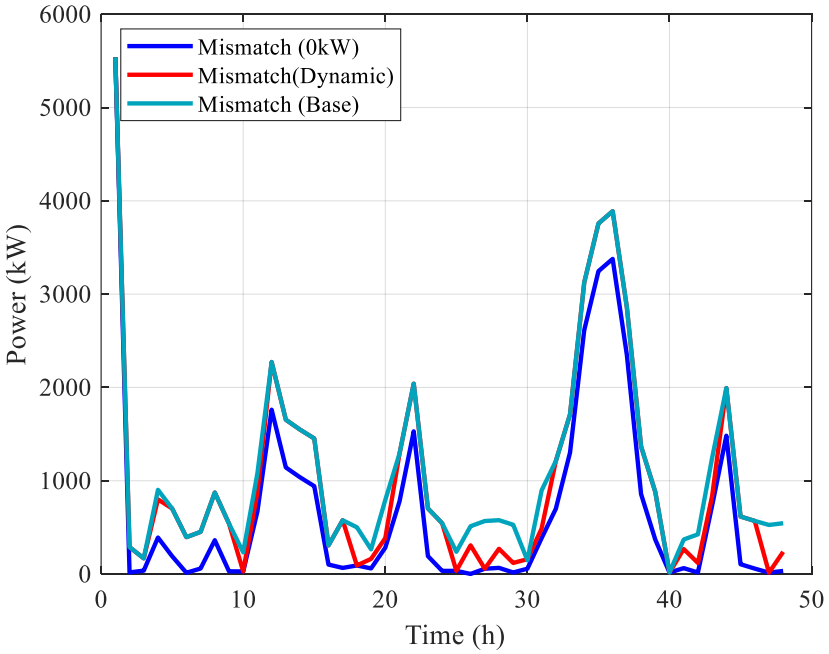

Fig. 70. Comparison of supply and demand mismatch after scheduling for different scenarios

Under the strict scenario (0 kW flexibility), demand must precisely match generation, resulting in higher scheduled and peak demand with a low average mismatch (693.99 kW) but many status changes (13,000). The base load scenario (500 kW static flexibility) smooths out demand, lowering peak demand (24,852.08 MW) and status changes (3,006) at the cost of a higher mismatch (1,118.64 kW). The dynamic scenario, which adjusts thresholds in real-time, achieves the lowest scheduled and peak demand (24,845.19 MW) and reduces energy consumption by 12.12%, striking a better balance with a moderate mismatch (1,012.41 kW).

6. CONCLUSION AND FUTURE WORK

This study introduced a novel rule-based peak shaving algorithm with a dynamic mismatch threshold designed to schedule refrigerators for peak demand management and maintain system stability in environments with limited generation capacity. The proposed algorithm operates within a framework that enables decision-making in both day-ahead and real-time scenarios to effectively schedule refrigerators. By utilizing historical data on demand and generation, the algorithm determines an optimal generation limit that system operators can aim to meet a day in advance. This generation limit is a key decision variable that informs the rules developed for the peak shaving algorithm, which adjusts the status of refrigerators in real time. Additionally, the algorithm uses day-ahead demand forecasts to anticipate peak and off-peak periods, allowing for dynamic adjustments that reduce peak demand during high-load periods and optimize excess generation usage during low-load times, thereby enhancing grid stability and balance. The effectiveness of the algorithm was evaluated using network data from the Spanish Transmission Service Operators (TSO) over four years, under various flexibility threshold scenarios. The analysis revealed significant insights into how different flexibility allowances impact demand response performance. The main findings are summarized as follows:

Strict No-Flexibility Threshold: In this scenario, where there is no flexibility allowance (0 kW mismatch threshold), the algorithm led to a notable increase in peak demand by 2.93% and a rise in total energy consumption by 6.73%. This outcome demonstrates the drawbacks of a strict mismatch threshold, which necessitates frequent switching of TCLs. This frequent switching increases operational stress and energy consumption, although it efficiently utilizes excess generation during off-peak periods. The results also indicate that while this approach minimizes the average demand-supply mismatch, it imposes challenges in precisely matching supply and demand, especially under stringent conditions.

Base Load Flexibility Threshold: With a higher mismatch allowance of 1000 kW, the peak demand showed a slight increase of 0.08%, and total energy consumption rose by 3.97%. While this scenario offers some improvement over the strict no-flexibility condition by reducing the total status changes and operational stress on appliances, it still results in higher

energy use. The increased flexibility helps better manage demand-supply alignment and reduce the frequency of TCL switching, suggesting that some flexibility can alleviate operational inefficiencies while still making effective use of excess generation during off-peak times.

Dynamic Flexibility Threshold: The dynamic mismatch threshold scenario yielded the best results, with a substantial reduction in peak demand by 4.25% and a slight decrease in total energy consumption by 0.59%. This indicates that incorporating dynamic flexibility can significantly optimize demand response and enhance energy efficiency. The algorithm also reduced the total status changes in TCLs to 3,000, highlighting decreased switching frequency and less operational stress on appliances. The higher average demand-supply mismatch in this scenario suggests a well-balanced approach to managing demand and supply, effectively accommodating variations in grid conditions.

The comparative analysis across these scenarios demonstrates the benefits of integrating dynamic flexibility into demand response strategies. The dynamic approach not only reduces peak demand and total energy consumption but also minimizes the operational impact on appliances, as evidenced by fewer status changes. These findings underline the potential for dynamic flexibility to enhance the effectiveness of demand response programs.

Future research will focus on incorporating dynamic flexibility thresholds into demand response programs that integrate renewable energy sources. By dynamically adjusting flexibility thresholds based on real-time network conditions, such programs can significantly improve peak demand management and energy efficiency. Utilities and policymakers are encouraged to adopt flexible demand response strategies that adapt to changing conditions, leveraging the benefits of dynamic flexibility to ensure a more resilient and efficient power grid.

REFERENCES

[1] *How much electricity does a refrigerator, dishwasher, and an electric car use? n.d.* https://blog.se.com/sustainability/2023/01/24/how-much-electricity-does-a-refrigerator-dishwasher-and-an-electric-car-use-we-did-the-math/ (accessed June 15, 2024).

[2] *The Future of Cooling – Analysis - IEA n.d.* https://www.iea.org/reports/the-future-of-cooling (accessed June 15, 2024).

[3] United States Population 2024 (Live) n.d. https://worldpopulationreview.com/countries/united-states-population (accessed June 15, 2024).

[4] Ghana Population (2024) - Worldometer n.d. https://www.worldometers.info/world-population/ghana-population/ (accessed June 15, 2024).

[5] Akasiadis C, Chalkiadakis G, *Mechanism Design for Demand-Side Management*. IEEE Intell Syst 2017; 32: 24–31. https://doi.org/10.1109/MIS.2017.6.

[6] Machado B, Castro MF, Bragança L. *European Union legislation for demand-side management and public policies for demand response*. IOP Conf Ser Earth Environ Sci 2019; 225:012064. https://doi.org/10.1088/1755-1315/225/1/012064.

[7] Rana MM, Atef M, Sarkar MR, Uddin M, Shafiullah GM. *A Review on Peak Load Shaving in Microgrid—Potential Benefits, Challenges, and Future Trend*. Energies (Basel) 2022;15. https://doi.org/10.3390/en15062278.

[8] Kristian M. *Demand response of heating and ventilation within educational office buildings*. n.d.

[9] Li H, Wang SJ. *Load Management in District Heating Operation*. Energy Procedia 2015; 75:1202–7. https://doi.org/10.1016/j.egypro.2015.07.155.

[10] Sweetnam T, Spataru C, Barrett M, Carter E. *Domestic demand-side response on district heating networks*. Building Research & Information 2019 ;47:330–43. https://doi.org/10.1080/09613218.2018.1426314.

[11] Guelpa E, Barbero G, Sciacovelli A, Verda V. *Peak-shaving in district heating systems through optimal management of the thermal request of buildings*. Energy 2017 ;137:706–14. https://doi.org/10.1016/j.energy.2017.06.107.

[12] Brundu FG, Patti E, Osello A, Giudice M Del, Rapetti N, Krylovskiy A, et al. *IoT Software Infrastructure for Energy Management and Simulation in Smart Cities*. IEEE Trans Industr Inform 2017;13:832–40. https://doi.org/10.1109/TII.2016.2627479.

[13] Van Oevelen T, Vanhoudt D, Johansson C, Smulders E. *Testing and performance evaluation of the STORM controller in two demonstration sites*. Energy 2020; 197:117177. https://doi.org/10.1016/j.energy.2020.117177.

[14] Vanhoudt D, Claessens BJ, Salenbien R, Desmedt J. *An active control strategy for district heating networks and the effect of different thermal energy storage configurations*. Energy Build 2018; 158:1317–27. https://doi.org/10.1016/j.enbuild.2017.11.018.

[15] Claessens BJ, Vanhoudt D, Desmedt J, Ruelens F. *Model-free control of thermostatically controlled loads connected to a district heating network*. Energy Build 2018; 159:1–10. https://doi.org/10.1016/j.enbuild.2017.08.052.

[16] Li H, Wang SJ. *Load Management in District Heating Operation*. Energy Procedia 2015; 75:1202–7. https://doi.org/10.1016/j.egypro.2015.07.155.

[17] Wernstedt F, Davidsson P, Johansson C. *Demand side management in district heating systems*. Proceedings of the 6th international joint conference on Autonomous agents and multiagent systems, New York, NY, USA: ACM; 2007, p. 1–7. https://doi.org/10.1145/1329125.1329454.

[18] Hossain J, Saeed N, Manojkumar R, Marzband M, Sedraoui K, Al-Turki Y. *Optimal peak-shaving for dynamic demand response in smart Malaysian commercial buildings utilizing an efficient PV-BES system*. Sustain Cities Soc 2024;101. https://doi.org/10.1016/j.scs.2023.105107.

[19] Mohamed AAR, Best RJ, Liu X, Morrow DJ. *A Comprehensive Robust Techno-Economic Analysis and Sizing Tool for the Small-Scale PV and BESS*. IEEE Transactions on Energy Conversion 2022; 37:560–72. https://doi.org/10.1109/TEC.2021.3107103.

[20] Pimm AJ, Cockerill TT, Taylor PG. *The potential for peak shaving on low voltage distribution networks using electricity storage*. J Energy Storage 2018; 16:231–42. https://doi.org/10.1016/j.est.2018.02.002.

[21] Mahmud K, Hossain MJ, Town GE. *Peak-Load Reduction by Coordinated Response of Photovoltaics, Battery Storage, and Electric Vehicles*. IEEE Access 2018; 6:29353–65. https://doi.org/10.1109/ACCESS.2018.2837144.

[22] Greenwood DM, Wade NS, Taylor PC, Papadopoulos P, Heyward N. *A Probabilistic Method Combining Electrical Energy Storage and Real-Time Thermal Ratings to Defer Network Reinforcement*. IEEE Trans Sustain Energy 2017; 8:374–84. https://doi.org/10.1109/TSTE.2016.2600320.

[23] Manojkumar R, Kumar C, Ganguly S, Gooi HB, Mekhilef S, Catalão JPS. *Rule-Based Peak Shaving Using Master-Slave Level Optimization in a Diesel Generator Supplied Microgrid*. IEEE Transactions on Power Systems 2023; 38:2177–88. https://doi.org/10.1109/TPWRS.2022.3187069.

[24] Riffonneau Y, Bacha S, Barruel F, Ploix S. *Optimal Power Flow Management for Grid Connected PV Systems With Batteries*. IEEE Trans Sustain Energy 2011; 2:309–20. https://doi.org/10.1109/TSTE.2011.2114901.

[25] Brundu FG, Patti E, Osello A, Giudice M Del, Rapetti N, Krylovskiy A, et al. *IoT Software Infrastructure for Energy Management and Simulation in Smart Cities*. IEEE Trans Industr Inform 2017; 13:832–40. https://doi.org/10.1109/TII.2016.2627479.

[26] THE 17 GOALS | Sustainable Development n.d. https://sdgs.un.org/goals (accessed September 4, 2024).

[27] Abbasimehr H, Shabani M, Yousefi M. *An optimized model using LSTM network for demand forecasting*. Comput Ind Eng 2020; 143:106435. https://doi.org/10.1016/j.cie.2020.106435.

[28] Mirjalili S, Mirjalili SM, Lewis A. *Grey Wolf Optimizer. Advances in Engineering Software* 2014; 69:46–61. https://doi.org/10.1016/j.advengsoft.2013.12.007.

[29] Violeau D, Fonty T. *Calculating the smoothing error in SPH*. Comput Fluids 2019; 191:104240. https://doi.org/10.1016/j.compfluid.2019.104240.

[30] *Hourly energy demand generation and weather* n.d. https://www.kaggle.com/datasets/nicholasjhana/energy-consumption-generation-prices-and-weather/data (accessed June 15, 2024).